



**HAL**  
open science

# Coupling between progressive damage and permeability of concrete: discrete modelling and experimental analyses

Gilles Pijaudier-Cabot, George Chatzigeorgiou, Abdelhafid Khelidj, Vincent Picandet

## ► To cite this version:

Gilles Pijaudier-Cabot, George Chatzigeorgiou, Abdelhafid Khelidj, Vincent Picandet. Coupling between progressive damage and permeability of concrete: discrete modelling and experimental analyses. Second International Symposium on Continuous and Discontinuous Modelling of Cohesive-Frictional Materials (CDM 2004), Sep 2004, Stuttgart, Germany. pp.119-130, 10.1201/9780203023631-10 . hal-04660581

**HAL Id: hal-04660581**

**<https://hal.science/hal-04660581v1>**

Submitted on 4 Sep 2024

**HAL** is a multi-disciplinary open access archive for the deposit and dissemination of scientific research documents, whether they are published or not. The documents may come from teaching and research institutions in France or abroad, or from public or private research centers.

L'archive ouverte pluridisciplinaire **HAL**, est destinée au dépôt et à la diffusion de documents scientifiques de niveau recherche, publiés ou non, émanant des établissements d'enseignement et de recherche français ou étrangers, des laboratoires publics ou privés.



Distributed under a Creative Commons Attribution - NonCommercial 4.0 International License

# Coupling between progressive damage and permeability of concrete: discrete modelling and experimental analyses

G. Pijaudier-Cabot

*R&DO – Institut GeM, Ecole Centrale de Nantes, France*

G. Chatzigeorgiou

*Dept. of Civil Engineering, Aristotle University of Thessaloniki, Greece*

A. Khelidj

*R&DO – Institut GeM, IUT de Saint Nazaire, France*

V. Picandet

*LG2M, Université de Bretagne Sud, France*

**ABSTRACT:** A significant increase of the permeability of concrete upon micro-cracking and a good correlation between the evolutions of damage (material stiffness) and permeability are observed experimentally. The present contribution investigates first this correlation theoretically, with the help of lattice analyses. Hydro-mechanical problems are considered with the construction of a hydraulic lattice, dual to the mechanical one. We observe that the average permeability upon micro-cracking is indexed on the evolution of the lattice compliance in the mechanical problem. Experimental results are reported in order to further quantify this growth of permeability due to damage.

## 1 INTRODUCTION

In large structures such as concrete nuclear vessels where the long term safety is of high priority, durability is important for design. Among the parameters playing a pivotal role, material permeability is one of the most important if one considers that vessels should not exhibit a leakage rate above a certain threshold whenever there is a sudden increase of pressure inside the vessel (for instance due to integrity tests). In most cases, apart from extremely severe accidents, mechanical loads induced by the increase of gas pressure inside the vessel yield moderate micro-cracking that can be viewed as distributed damage. Therefore, simulations of such case studies, with the aim of estimating the increase of leakage rate that is induced by internal pressure in vessels, ought to rely on continuum material models in which the evolution of material permeability is related to the non linear mechanical response of concrete.

In tension or compression (and for moderate confining pressures), concrete fails due to micro-crack propagation and coalescence. Micro-cracks, whose development at the beginning is almost homogeneously distributed, start to concentrate in a region inside the material as the peak load is approached. Failure occurs with a sudden propagation of one or more macro-cracks. With the increase of cracking there is also a decrease of the stiffness of the material. In damage models this reduction of stiffness is expressed through a damage parameter (see e.g. Mazars and Pijaudier-Cabot, 1989; Pijaudier-Cabot and Jason, 2002).

Experimental results have shown that for low and intermediate stress levels (diffuse distribution of damage), the permeability of concrete to water (Kermani, 1991; Hearn, 1999) or gas (Sugiyama

et al., 1996) exhibits a slow increase (typically of one order of magnitude at the most), and then increases dramatically by several orders of magnitude when the load is very close to the ultimate strength of the material and further in the softening regime. From a microscopic point of view, in the first regime up to the peak load (Wang et al., 1997), the width of the cracks is relatively small. Micro-cracks do not form a connected network. In the second regime, a macro-crack forms and the transfer properties of the structure become almost solely governed by the macro-crack opening and tortuosity (the permeability of the surrounding material is so small that its effect is negligible). In this contribution, we are interested in the first regime of relatively slow growth of permeability, as major through macro-cracks are not expected to occur in vessels. We look at modelling the relationship between micro-cracking and permeability in a material that can still be viewed as a continuum with a homogeneous (or slowly varying) distribution of micro-cracks.

Coupling between the non linear response of concrete and its permeability can be achieved in a very standard way with the help of the theory of porous materials initially due to Biot (see e.g. Biot 1941; Coussy, 1995). This approach has become very popular in the literature for durability analyses involving mass transfer such as hydro-mechanical damage analyses (Bary et al., 2000), analysis of concrete at an early age (Ulm and Coussy, 1996), chemo-mechanical effects (Ulm et al., 1999), and more generally environmentally induced degradations (Bangert et al., 2003). In these approaches, however, the relationship between the material permeability and the degradation induced in the material due to mechanical loads is phenomenological. Theoretical investigations of such relationships are relatively recent in the context of cement-based materials. They rely on homogenisation techniques (Dormieux and Lemarchand, 2001; Dormieux and Kondo, 2004) where the distribution of micro-cracks needs to be characterised accurately (size, shape, opening, orientation). Such approaches provide a justification of the expected relationship between the crack density and the permeability. The applied effective stress may also play a role as far as the propagation of these micro-cracks is concerned.

Another approach, which serves the same purpose as homogenisation techniques, is the scaling analysis of discrete lattices. Simple discrete models were used in the past in order to study the failure of heterogeneous materials. Two dimensional lattices consisting of beams (Herrmann et al., 1989) or springs (Hansen et al., 1989) have been used, where the heterogeneity is captured by a random distribution of the failure thresholds of each beam/bar. Although these lattices are very simple, and not capable of reproducing the exact features of the micro-cracking processes in brittle heterogeneous materials, the limit of a lattice of infinite size is quite relevant as it is related to the response of a material point in the continuum sense. Hence, there is an interest at studying the scaling properties of such lattices, and in particular the characteristics that describe the lattice in a size independent way. Such quantities are those that are expected to be found in a continuum model, as representatives of the material degradation. Following this technique, Delaplace et al. (1996) have shown that a proper way to capture material damage due to micro-cracking, described as the failure of elastic brittle bonds in a discrete model, is to model the variation of the material stiffness in a continuum setting (which can then be indexed by a damage variable). A similar observation has been also reported by Krajcinovic and Basista (1991).

In this paper, we attempt the same type of approach with the aim of investigating the variation of material permeability due to mechanical damage and their relationship. We start with the mechanical analysis. We recall the main features of the study performed by Delaplace et al. (1996), extending the analysis to lattices of larger sizes with a more representative statistical analysis. Hydro-mechanical coupling is then performed by superimposing two lattices: one for the mechanical problem and a second one for the hydraulic problem. We find that the hydraulic problem is described by the overall variation of stiffness observed in the mechanical problem. Therefore, the material permeability should indeed be correlated to continuum damage (and not to the applied stress for instance). Finally we report some experimental results in which the evolution of permeability of concrete subjected to various increasing loads at 2 different temperature is obtained. We compare also the results from the theoretical analysis with experimental curves obtained by Picandet et al. (2001), from a qualitative point of view.

## 2 MECHANICAL PROBLEM

The lattice which will be described in the following was used in the past for the study of the failure mechanism of quasi-brittle materials (see Krajcinovic and Van Mier (2000) or Delaplace et al. (1996) for complete details). It is a stiffness controlled model, where the mechanical problem is substituted by an electrical analogous, simplifying the analysis by transforming it from vectorial to scalar. As shown by De Arcangelis et al. (1989), this simplification is able to capture the most important physical aspects of the problem with a simpler approach. The model, which is depicted in Figure 1, is a regular two-dimensional lattice whose bonds are one dimensional. The lattice size is  $L \times L$  where  $L$  is related to the total number of bonds  $n = 2L^2$ . Instead of solving the mechanical problem, we solve an electrical analogous substituting the strain  $\epsilon$  with the voltage difference  $v$ , the stress  $\sigma$  with the current  $i$ , and the Young's Modulus  $E$  with the conductance  $G$ . So, we substitute the constitutive equation:

$$\sigma = E \cdot \epsilon \quad (1)$$

with:

$$i = G \cdot v \quad (2)$$

The boundary conditions of the model are periodic in order to avoid boundary effects. They represent a homogeneous loading in the vertical direction: Periodicity is imposed along the boundaries parallel to the vertical axis and a constant unit jump of voltage is applied between the horizontal boundaries.

Every bond of the lattice behaves as a brittle material which has a conductance equal to 1. When it reaches a threshold current  $i_c$ , it fails.  $i_c$  differs from bond to bond following a uniform random distribution between 0 and 1.

We start the calculation by assigning a threshold current to every bond with the help of a random generator number (Press et al., 1992). At each step, the algorithm computes the voltage at each node from Kirchoff's law. The equations form a symmetric band matrix which is solved using Cholesky factorisation. From Ohm's law, the current of each bond is obtained. The bond which fails first is the one which has the minimum ratio of its strength  $i_c$  to its current. This bond is removed from the lattice by changing its conductance from 1 to 0. Because the analysis is linear, it is also possible to compute the overall load (intensity) at which this bond fails and the process continues with the next step of loading where we look at the next bond which fails. Figure 2 shows a typical current versus voltage response (lattice of size 64). The snapbacks in Figure 2 are observed because the load process is stiffness controlled. In a displacement controlled scheme, the envelope of the curve would be recovered only.

The lattice does not represent a real material. In fact, we are interested in its scaling properties: as the lattice size tends to infinity, its response tends to a thermodynamic limit which is the response of a single point in a continuum approach. Hence, we shall look at the variables that are capable to describe the evolution of the lattice response with bond breakage, independently from its size.

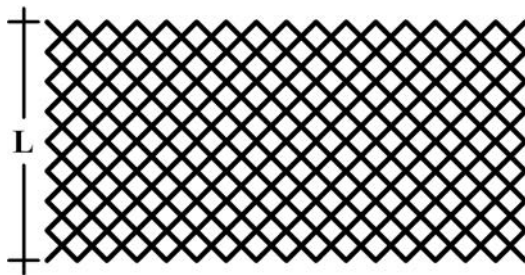


Figure 1. Lattice model.

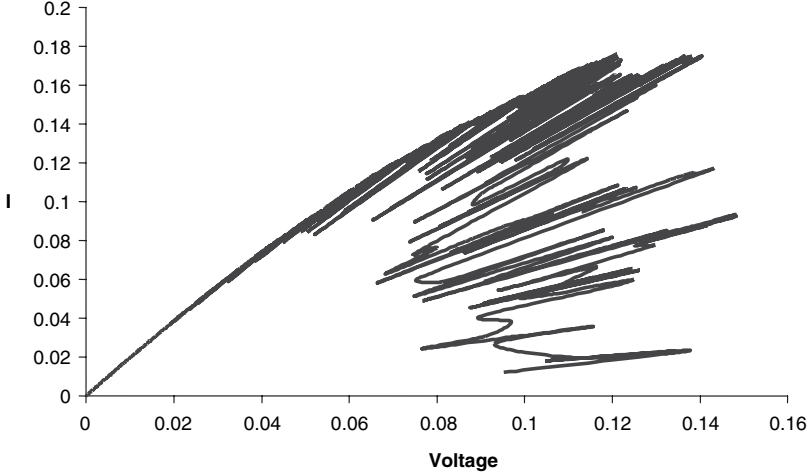


Figure 2. Typical intensity (load) versus voltage (relative displacement) response of a lattice of size 64.

These are the variables that should characterise the continuum point response, those which should enter in a continuum formulation, whatever the phenomenological details or the continuum model chosen.

In the mechanical problem, we characterise the distribution of local currents with the evolution of the lattice degradation (bond failures). For this, we introduce the moments which are calculated according to the formula:

$$M_m = \int i^m N(i) di \quad (3)$$

where  $i$  is the current of each bond,  $N(i)$  is the number of bonds whose current is in the range of  $[i, i+di]$ , and  $m$  is the order of moment. We limit the analysis to moments of order up to 4. This assumption is equivalent to a truncation in a series. The zero order moment is the number of unbroken bonds, the first order moment is proportional to the average value of the current. The second order moment is proportional to the overall conductance  $\bar{G}$  of the lattice (stiffness in the mechanical problem):

$$M_2 = \int r i^2 N(i) di = 2\bar{G}v^2 = 2\bar{G} \quad (4)$$

where  $r$  is the local resistance of the bond (unit resistance here) and the voltage difference applied to the lattice is equal to 1. Note that the fourth order moment is a measure of the dispersion of conductance.

As each lattice has a unique distribution of bond thresholds, several computations with different random seeds must be performed in order to achieve a representative statistical treatment of the results for which useful conclusions about the average behaviour of the lattice can be made. Figure 3 represents the average moments of 300 different random seeds for different lattice sizes as a function of the moment of order 2 until the peak current.

In these diagrams, and in all further similar figures, every curve represents, in a logarithmic scale, the opposite of the moments divided by their value at the beginning of the calculation (no damage). Hence, the zero order moment increases as the number of unbroken bonds decreases and the second order moment increases as the overall conductance decreases. We can observe that until the peak, the curves of  $M_0$ ,  $M_1$ ,  $M_2$  and  $M_3$  versus  $M_2$  are independent from the size of the lattice approximately. Hence, the average conductance is a parameter that describes the distribution of current and its evolution due to bond breakage, whatever the size of the lattice. It means

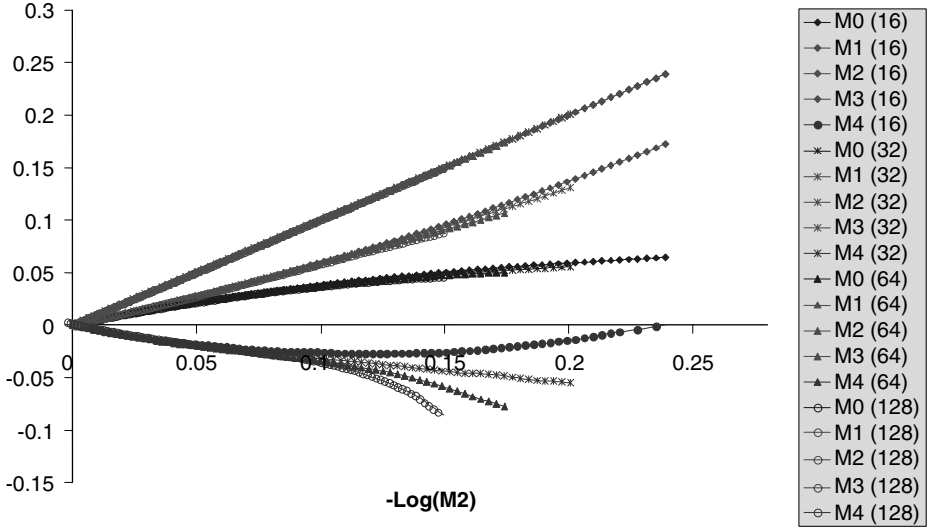


Figure 3. Opposite of the logarithm of the moments of order 0 to 4 as a function of the opposite of the logarithm of the moment of order 2 in the mechanical problem for lattice sizes ranging from 16 to 128.

also that the overall degradation of conductance (stiffness) is the parameter which represents local bond breakage in the continuum approach. This is consistent with what was observed by Delaplace et al. (1996), with lattices ranging from size 8 to 64, with a limited number of runs (30) for the larger lattice. It was also shown that the number of broken bonds (e.g. the micro-crack density in a continuum model) could not characterise the state of damage in a size independent way. Here, each data set for one lattice size is comprised of 300 runs and lattices of size 128 could be computed too.

### 3 LATTICE MODEL FOR THE HYDRO-MECHANICAL PROBLEM

In order to represent the influence of material damage on the permeability, it is reasonable to assume that when a bond fails in the mechanical lattice, it opens a larger path for fluid flow in the perpendicular direction (we do not consider here mechanical damage due to hydraulic pressure). This basic scheme is depicted in Figure 4. The hydraulic lattice is build following this principle, with bonds that are perpendicular to the mechanical lattice.

The periodicity of the mechanical lattice yields the hydraulic dual lattice shown in Figure 5 called the sister lattice (to the mechanical one). As mentioned by Dormieux and Kondo (2004), the fluid flow at the micro-scale level (bond level) can be described by Darcy equation:

$$q = K \cdot \nabla p \quad (5)$$

where  $q$  is the flow rate,  $\nabla p$  is the drop of pressure  $p$ , and  $k$  is the local permeability. We are going to assume that when a bond fails, the local permeability in the perpendicular direction is increased by an amplification factor  $k$  which is very large, typically of the order of  $10^{-6}$ .

Again, periodic boundary conditions are applied to the hydraulic lattice and we use an electrical analogy. This means that the voltage represents the pressure  $p$ , the current represents the flow rate  $q$  and the conductance represents the permeability  $k$ . A constant drop of pressure equal to 1 is applied at the vertical boundaries of the lattice. At each step of damage in the mechanical lattice, the flow rate is computed in the sister lattice and the various moments of its distribution are computed too.

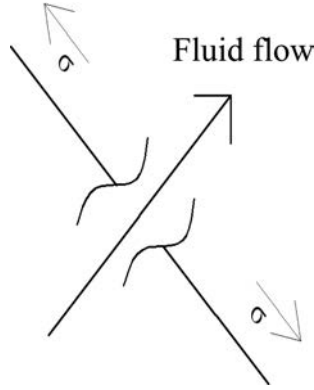


Figure 4. Basic scheme for the coupled hydro-mechanical lattice analysis. When a mechanical bond fails, the permeability of a perpendicular bond increases suddenly.

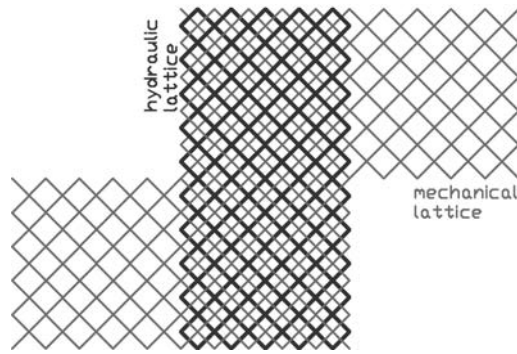


Figure 5. The mechanical and the hydraulic lattices.

It is worthwhile to point out that the hydro-mechanical coupled effect is introduced at the local scale, same as the degradation process in the mechanical problem. Furthermore, we analyse here the permeability of the unloaded material. Same as in classical poro-mechanics, there is no effect of the applied stress on the permeability in the reversible regime and it cannot be expected to be observed in the present computations. What we intend to see is on which parameter of the mechanical problem the variation of permeability depends, and by which moment of the mechanical problem the evolution of the fluid flow distribution in the lattice can be described in a size independent way. Following the same technique as in the mechanical problem, we look at the moments of the distribution of the hydraulic flow rate, and we try to find for which moment of the distribution of the local stress (current) the plots collapse on the same curve for different sizes.

The second order moment in the mechanical problem is a natural candidate since it is this one which describes the evolution of mechanical damage. Figure 6 shows the plot of the moments of order 1, 2 and 4 in the hydraulic lattice as a function of the moment of order 2 in the mechanical lattice. The collapse of the evolution of the moments of order 1 and 2 for lattice sizes ranging from 16 to 128 is quite satisfactory when  $-\log(M_2)$  for the mechanical problem is less than 0.1 (same as in Figure 3).

We may conclude that the evolution of the distribution of the local flow rates due to mechanical bond failure is described by the variation of stiffness due to the mechanical degradation in the mechanical problem, whatever the lattice size when the amount of damage is moderate (moment

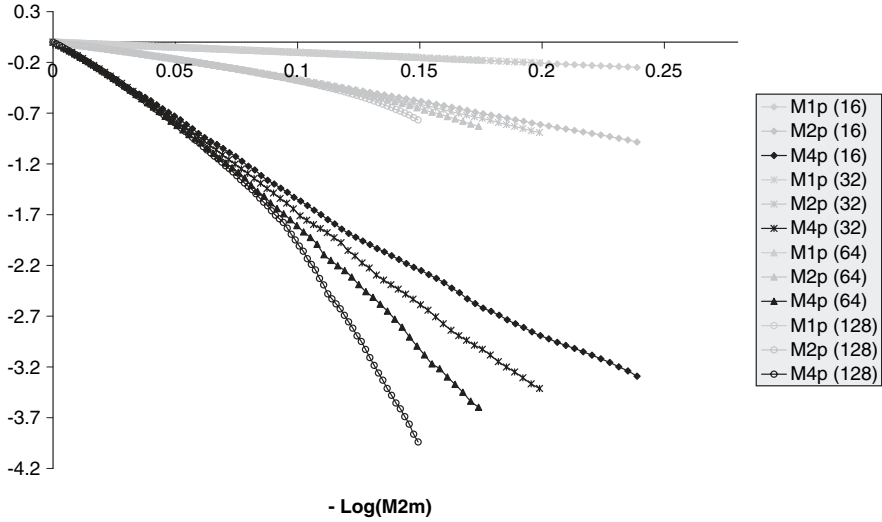


Figure 6. Opposite of the logarithm of the moments of order 1, 2, 4 in the hydraulic problem as a function of the opposite of the logarithm of the moment of order 2 in the mechanical problem for lattice sizes ranging from 16 to 128.

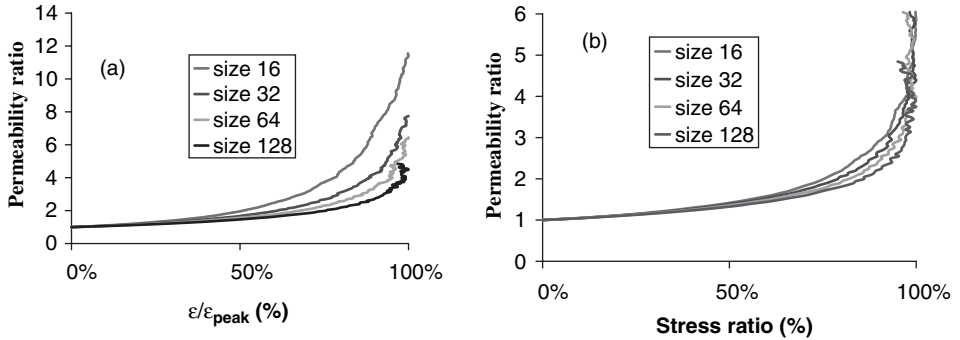


Figure 7. Permeability divided by the initial permeability versus strain (a) and stress (b) ratios to the peak for various lattice sizes.

of order 2 ranging from 0 to 0.1 or 0.15 approximately). In this regime and in the limit of a continuum model, for an infinite lattice size, the variation of material permeability due to bond breakage (micro-cracks) should be controlled by the degradation of stiffness in the mechanical problem, and not by the number of broken bonds (local degradation), the overall strain or the average stress. Figure 7 shows the plots of the evolution of the average permeability divided by the initial permeability (derived from the moment of order 2 in the hydraulic problem), as a function of the applied strain or the applied stress in the mechanical problem. These quantities should be seen here as history variables: the curves show the evolution the average permeability as a function of the maximum strain (stress) reached during the loading history. We can see that for each size of lattice a different curve is obtained.

By comparison, Figure 8 shows the evolution of the permeability as a function of the evolution of stiffness in the mechanical lattice. For all the sizes considered, the plots collapse onto the same curve for stiffness variations ranging from 0 to 0.2 approximately, before the peak load. For large variations of the stiffness, lattices have entered far in the softening regime and the lattice size starts



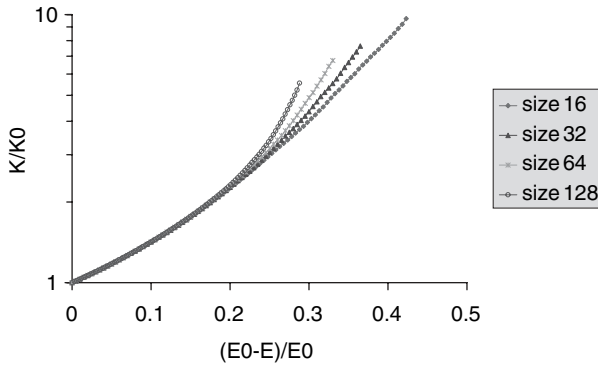


Figure 8. Permeability versus Young Modulus reduction according to the lattice analysis.

to play an important role because it controls the spacing between the macro-cracks. Therefore, results cannot be interpreted properly in this regime.

#### 4 EXPERIMENTAL DATA

Experimental results have shown that for low and intermediate stress levels, the water or the gas permeability of concrete has insignificant variations, but that it increases very fast when the load is very close to the ultimate strength of the material. From a microscopic point of view the width of the micro-cracks is relatively small up to the peak load, but increases radically in the softening regime, causing a tremendous change in the permeability. In the pre-peak regime, it seems that it is rather the number of micro-cracks and not their openings that is important. Experimental tests have also shown that when the temperature increases up to 80°C the relative water permeability has a slight increase and the self healing process of concrete becomes faster.

We start here by reporting test data from an experimental study which is still in progress. Cylindrical hollow specimens made of concrete are subjected to stress ratios between 20 and 95% of the maximum stress. The radial gas (nitrogen) permeability is measured during the test, as a function of the applied load. The gas enters the specimen through the longitudinal central hole in the specimen and exits radially from its perimeter. Thereafter it is concentrated in an elastic membrane and is led to a flowmeter. From the outgoing flux, the intrinsic material permeability is computed. Furthermore, the set-up is placed in a climate control chamber where the temperature and the humidity is controlled. Figure 9 shows a schematic view of the test set-up.

Eight specimens have been tested up to now at ambient temperate (20°C) and at 40°C. These are cylinders of diameter 11 cm and height 22 cm. The internal diameter of the hollow cylinders is 1.4 cm. Figure 10 shows the specimen tested.

Prior to the test, the specimens have been cured in water for 28 days and dried in an oven at 105°C for three months so that the saturation index of the material is in the range of a few percents.

The variation of permeability of two specimens is shown in Figures 11 and 12. These data are typical results recorded at ambient temperature and at 40°C. Note that it is the variation of intrinsic permeability measured *under load* that is reported here, as opposed to many existing test data and to the above theoretical analysis. On these diagrams, the permeability is multiplied by 3 approximately as the load is increased. The increase is measured for load levels that are higher than the threshold of damage (70% of the maximum load approximately). It suggests that this phenomenon is due to the growth of micro-cracks (vertical micro-cracks mainly in a compression test). A slight decrease of permeability is often observed at the beginning of the test. It corresponds probably to initial micro-cracks or micro-pores closure.

These test data are similar to those by Sugiyama et al. (1996). They conducted experiments on different normal-weight concretes and different light-weight concretes with the same water/cement

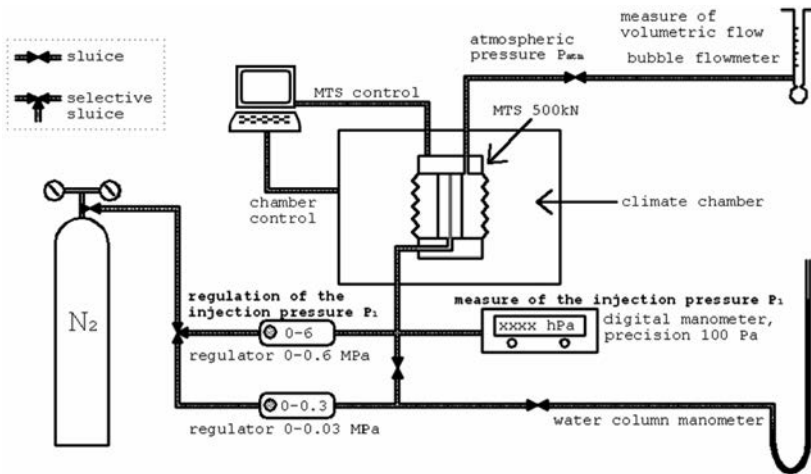


Figure 9. Schematic description of the test set-up.

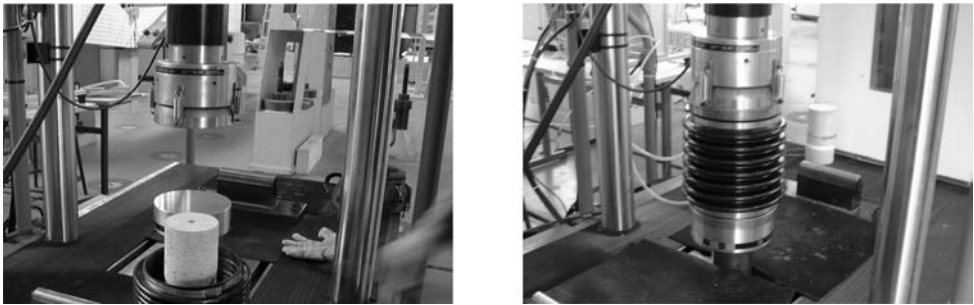


Figure 10. Specimen placed in the testing machine.

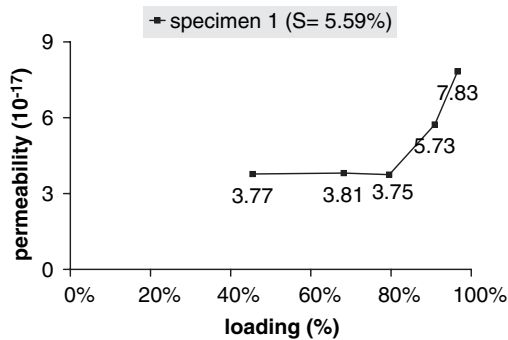


Figure 11. Variation of intrinsic permeability ( $m^2$ ) under load for concrete at ambient temperature.

ratios. One cannot say that very different test data have been obtained for 20°C and 40°C. The influence of the temperature is within the dispersion of experimental data. It seems, however, that the relative increase of permeability at 40°C is a bit higher than at ambient temperature.

During the tests, permeability upon unloading could not be obtained. Therefore, it is quite difficult to correlate the data with the decrease of stiffness due to damage that is expected from

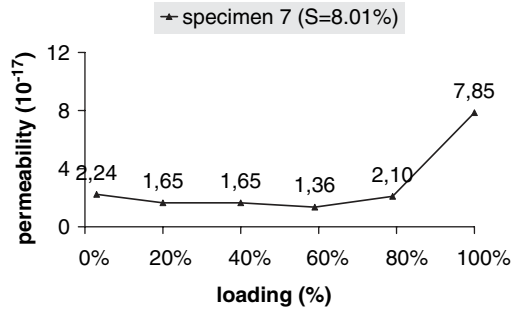


Figure 12. Variation of intrinsic permeability ( $m^2$ ) under load for concrete under load at  $40^\circ C$ .

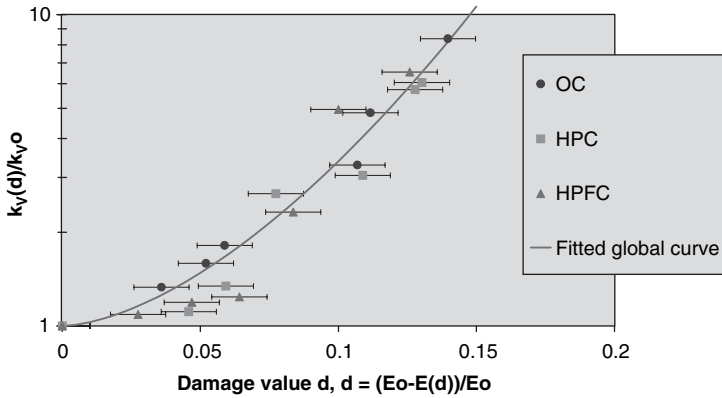


Figure 13. Permeability versus Young Modulus reduction: experimental data from Picandet et al. (2001).

the theoretical analysis without assuming that the variation of permeability upon unloading is negligible. However, some comparable data can be found in the literature. Picandet et al. (2001) investigated the variation of permeability of several types of concretes. The gas permeability was measured on circular discs taken from compression cylinders, loaded at different stresses in the pre-peak regime, after the specimens were dried.

Figure 13 shows the experimental data. Qualitatively, the experiments and the lattice analysis provide the same result. Experimentally, the evolution of the permeability with the applied stress (or strain) depends upon the type of material tested. The fact that the variation of permeability recorded experimentally does not depend on the type of concrete tested (ordinary concrete – OC, high performance concrete – HPC, high performance fiber reinforced concrete – HPFC) tends to demonstrate that there is an intrinsic relationship between the permeability and the evolution of the material stiffness indexed by a damage variable. The same type of relationship is recovered from the lattice analysis theoretically, in the regime of moderate micro-cracking.

## 5 CLOSURE

In this paper, we have studied the mechanical and the hydro-mechanical responses of quasi-brittle materials, focusing in concrete, using a lattice model. In the mechanical problem, the influence of material degradation (bond breakage) is described by the evolution of the material stiffness of the lattice. The hydro-mechanical problem is analysed by construction of a sister lattice. When a bond breaks in the mechanical lattice, it increases the permeability of a bond in the hydraulic lattice

bond that is perpendicular to the first one. The analysis of the lattice results follows the technique implemented in the mechanical problem. The various moments of the flow rate distribution are computed and we look for the variable that describes the evolution of these moments independently from the size of the lattice. If such a quantity is found, it is the quantity that describes the evolution of the flow rate distribution with material degradation.

- The permeability of the lattice increases progressively with the increase of material degradation. The average stiffness constructs lattice size independent relations with the hydraulic moments of order up to 4, for a moderate material degradation, before the peak load is reached.
- Experiments at ambient temperature and at 40°C have been reported. In the regime of progressive damage, when the specimen has not entered the softening regime, a moderate increase of permeability is observed with the applied load. From the literature, it is also observed that the increase of permeability can be consistently correlated with the unloading stiffness of the specimen (or the variation of stiffness).

As a consequence, it is clear that in continuum poro-mechanics, the material permeability should be related to the degradation of stiffness (and of course the degree of saturation too when one deals with gas permeability). It underlines also the need for a proper description the material stiffness degradation whenever hydro-mechanical problems are considered (Jason et al. 2004).

## ACKNOWLEDGEMENTS

Financial supports from the network on Degradation and Instabilities in Geomaterials with Application to Hazards Mitigation (DIGA), contract HPRN-CT-2002-00220 with the European Commission and from the partnership between EDF and the R&DO group are gratefully acknowledged.

## REFERENCES

- Bangert F., Grasberger S., Kuhl D., and Meschke G., Environmentally Induced Deterioration in Concrete: Physical Motivations and Numerical Modeling, *Engrg. Fract. Mech.*, vol. 70, pp. 891–910, 2003.
- Bary B., Bournazel J.P., and Bourdarot E., Poro-Damage Approach Applied to Hydro-Mechanical Fracture Analysis of Concrete, *J. Engrg.Mech. ASCE*, vol. 126, pp. 937–943, 2000.
- Biot M.A., General Theory of Three-Dimensional Consolidation, *J.Applied Phys.*, vol. 12, 155–165, 1941.
- Coussy O., *Mechanics of Porous Continua*, John Wiley Interscience, 1995.
- De Arcangelis L., Herrmann H. J., Scaling and Multiscaling Laws in Random Fuse Networks. *Physical Reviews B*, 1989, vol. 39, No. 4, pp. 2678–2684.
- Delaplace A., Pijaudier-Cabot G., Roux S., Progressive damage in discrete models and consequences on continuum modeling. *Journal of Mechanics and Physics of Solids*, 1996, vol. 44, No. 1, pp. 99–136.
- Dormieux L. and Lemarchand E., Homogenization Approach of Advection and Diffusion in Cracked Porous Materials, *J. Engrg.Mech. ASCE*, vol. 127, pp. 1267–1274, 2001.
- Dormieux L. and Kondo D., Approche micromécanique du couplage perméabilité endommagement, *C.R.Mécanique*, vol. 332, pp. 135–140, 2004.
- Hansen A., Roux S., Herrmann H. J., Rupture of Central-Force Lattices. *J. Physique*, 1989, vol. 50, pp. 733–744.
- Hearn N., Effect of Shrinkage and Load-Induced Cracking on Water Permeability of Concrete. *ACI Materials Journal*, 1999, vol. 96, No. 2, pp. 234–241.
- Herrmann H. J., Hansen A., Roux S., Fracture of disordered, elastic lattices in two dimensions. *Physical Review B*, 1989, vol. 39, pp. 637–648.
- Jason L., Pijaudier-Cabot G., Huerta A., Crouch R. and Ghavamian S., An Elastic Plastic Damage Formulation for the Behaviour of Concrete, *Proc. Francos 5*, V. Li et al. Eds., Vail, April 2004.
- Kermani A., Permeability of stressed concrete. *Building research and information*, 1991, vol. 19, No. 6, pp. 360–366.

- Krajcinovic, D. and Basista M., Rupture of Central Force Lattices Revisited, *J. Physique*, Vol. 1, pp. 241–245, 1991.
- Krajcinovic, D. and Van Mier J.G.M., Damage and Fracture of Disordered Materials, *CISM courses and lectures* No. 410, 2000.
- Mazars J. and Pijaudier-Cabot G., Continuum Damage Theory : Application to Concrete, *Journal of Engrg. Mech.* ASCE, Vol. 115, No 2, pp. 345–365, 1989.
- Picandet V., Khelidj A., Bastian G., Effect of axial compressive damage on gas permeability of ordinary and high-performance concrete. *Cement and Concrete Research*, 2001, vol. 31, pp. 1525–1532.
- Pijaudier-Cabot G., Jason L., Continuum damage modelling and some computational issues. In *Revue française de genie civil*, volume 6 – No 6, 2002, pp. 991–1017.
- Press W. H., Teukolsky S. A., Vetterling W. T., Flannery B. P., *Numerical Recipes in FORTRAN 77: The Art of Scientific Computing*. Cambridge University Press, 1992.
- Sugiyama T., Bremner T. V., Holm T. A., Effect of Stress on Gas Permeability in Concrete. *ACI Materials Journal*, 1996, vol. 93, No. 5, pp. 443–450.
- Wang K., Jansen D. C., Shah S. P., Karr A. F., Permeability study of cracked concrete. *Cement and Concrete Research*, 1997, vol. 27, No. 3, pp. 381–393.
- Ulm F.J. and Coussy O., Strength Growth as Chemo-Plastic Hardening in Early Age Concrete, *J. of Enrg. Mech.* ASCE, 122, 1123–1132, 1996.
- Ulm F.J., Torrenti J.M., and Adenot F., Chemoporoplasticity of Calcium Leaching in Concrete, *J. of Enrg. Mech.* ASCE, 125, 1200–1211, 1999.